ELSEVIER

Biophysical Chemistry 125 (2007) 254–259

Biophysical Chemistry

http://www.elsevier.com/locate/biophyschem

Two-state irreversible thermal denaturation of *Euphorbia characias* latex amine oxidase

Mojtaba Amani [a], Ali A. Moosavi-Movahedi [a,*], Giovanni Floris [b], Anna Mura [b], Boris I. Kurganov [c], Faizan Ahmad [d], Ali A. Saboury [a]

[a] *Institute of Biochemistry and Biophysics, University of Tehran, Tehran, Iran*
[b] *Department of Applied Sciences in Biosystems, University of Cagliari, Cagliari, Italy*
[c] *Bakh Institute of Biochemistry, Russian Academy of Sciences, Leninskii prospect 33, Moscow, Russia*
[d] *Department of Biosciences, Jamia Millia Islamia, New Delhi, India*

Received 11 May 2006; received in revised form 7 August 2006; accepted 17 August 2006
Available online 23 August 2006

Abstract

Thermal denaturation of *Euphorbia* latex amine oxidase (ELAO) has been studied by enzymatic activity, circular dichroism and differential scanning calorimetry. Thermal denaturation of ELAO is shown to be an irreversible process. Checking the validity of two-state it really describes satisfactorily the thermal denaturation of ELAO. Based on this model we obtain the activation energy, parameter T^* (the absolute temperature at which the rate constant of denaturation is equal to 1 min^{-1}), and total enthalpy of ELAO denaturation. HPLC experiments show that the thermal denatured enzyme conserves its dimeric state. The $N_2 \xrightarrow{k} D_2$ model for thermal denaturation of ELAO is proposed: where N_2 and D_2 are the native and denatured dimer, respectively.

Keywords: Copper containing amine oxidase; Differential scanning calorimetry; Kinetic models; Irreversible denaturation

1. Introduction

Cu/TPQ amine oxidases (AOs; E.C. 1.4.3.6) are a group of heterogeneous dimeric enzymes, each subunit containing one Cu (II) and one 2,4,5-trihydroxyphenyalanine quinone (TPQ) as cofactors. TPQ is formed from a posttranslational self-processing of a tyrosine residue [1] in the amino acid sequence. These enzymes catalyze the oxidative deamination of primary amines to the corresponding aldehydes, hydrogen peroxide, and ammonia.

AOs are widely distributed in nature, occurring in plants, microorganisms, and mammals [2]. Although the functional role of Cu/TPQ AOs has not been clearly determined, it has been shown that plasma level of amine oxidases varies in diabetes [3], heart failure [4], patients suffering from serious burns and solid tumors, pregnancy and age [5]. In microorganisms these enzymes have nutritional role using primary amines as a sole source of nitrogen or carbon. In plants AOs can play a role in regulating intercellular polyamine levels, morphogenesis [6], and mobilization of seed reserves [7]. The level of plant AOs changes upon auxin treatment [8], light stress [9], germination [10], anoxic and thermal stress [11], salt stress [12], and mechanical injury [13].

In spite of intensive physiological and pharmaceutical studies on Cu/TPQ AOs, there are very few literature surveys on the thermodynamics of this group of enzymes. Moosavi-Nejad et al. [14] reported that thermal denaturation of lentil seedling amine oxidase (LSAO) showed two main reversible peaks, the first broad while the second one relatively sharp. They also deconvoluted the second peak to three subpeaks and supposed that subpeaks belonged to three hypothetical structure domains for each subunit of LSAO.

Giartosio et al. [15] analyzed thermal denaturation of bovine serum oxidase (BSAO) by differential scanning calorimetry (DSC). These authors showed that the DSC profile of BSAO had three distinct peaks. The thermogram of BSAO was deconvoluted

Abbreviations: BSAO, bovine serum amine oxidase; DSC, Differential scanning calorimetry; ELAO, *Euphorbia latex* amine oxidase; PSAO, pea seedlings amine oxidase; TPQ, 2,4,5, trihydroxyphenylalanine quinone.

* Corresponding author. Tel.: +98 21 66403957; fax: +98 21 66404680.
E-mail address: moosavi@ibb.ut.ac.ir (A.A. Moosavi-Movahedi).

0301-4622/$ - see front matter © 2006 Elsevier B.V. All rights reserved.
doi:10.1016/j.bpc.2006.08.006

to four two-state independent transition albeit they did not mention whether this process was reversible or not. In a successive study the same authors deconvoluted the thermogram to five two-state transitions [16] explaining discrepancies rising from some protein impurity. Moreover they reported that transitions 1 and 5 showed reversibility.

The aim of the present work is to study the thermal denaturation of amine oxidase from *Euphorbia characias* latex (ELAO) by different methods and to propose a model of thermal denaturation of the protein.

2. Material and methods

2.1. Protein purification

ELAO was purified by the procedure described in [17]. Only protein of the highest quality was utilized on the basis of 2.0± 0.1 titratable TPQ/dimer.

An ε_{278} of 3.78×10^5 $M^{-1}cm^{-1}$ was used to determine the protein concentration [18].

2.2. Enzyme assay

ELAO activity was measured by the oxidation of guaiacol in the presence of hydrogen peroxide and horseradish peroxidase. The reaction mixture contained 100 mM potassium phosphate buffer, pH 7.0, 13 mM putrescine as a substrate, 0.1 U/ml horseradish peroxidase and 0.5 mM guaiacol in a final volume of 1 ml. The increase in absorbance at 470 nm was recorded using a Cary 100 UV–visible Spectrophotometer (Varian, Australia) at 27 °C. For studying the thermal denaturation of ELAO in terms of enzymatic activity, the *Euphorbia* enzyme (8×10^{-9} M) in 100 mM phosphate buffer, pH 7.0, was incubated for 20 min at desired temperature and then cooled to 27 °C to measure the activity. Reported activity values are the activities relative to native enzyme at 27 °C and are the mean of at least three different measurements.

2.3. Circular dichroism experiments

CD spectral measurements in far-UV regions were made on Aviv model 215 (USA) CD–spectropolarimeter equipped with a water-bath circulating system using 0.1-cm path length cuvettes. Protein concentration was typically 0.25 mg/ml.

2.4. Determination of aggregation state

ELAO was denatured by heating up to 90 °C and then cooled to 27 °C. For detection of aggregation, absorbance of native and denatured ELAO was recorded using Cary 100 UV–visible Spectrophotometer in the range 200–500 nm at 27 °C.

2.5. Calorimetric study

Calorimetric studies were carried out by a Scal-1 differential scanning microcalorimeter (Russia) equipped with 0.355 ml capillary glass cells. All DSC experiments were done under 2 atm pressure. The concentrations of ELAO were 0.5–4.0 mg/ml. The experiments were performed at scan rates 0.125, 0.25, 0.475, and 1 °C/min.

2.6. Data analyses

Irreversible protein denaturation is thought to have at least two steps:

a) reversible unfolding of the native protein,
b) irreversible alteration of the unfolded protein to final state that is unable to fold back to native state.

This model is known as a Lumry–Eyring model and can be shown as:

$$N \underset{k_{-1}}{\overset{k_1}{\rightleftharpoons}} U \xrightarrow{k} F \qquad \text{(SchemeI)}$$

where N, U, and F indicate native, unfolded, and final state of the protein; $\underline{k}_1$, $\underline{k}_{-1}$, and $\underline{k}$ are the rate constants for reversible denaturation, renaturation, and irreversible denaturation stage, respectively. If $\underline{k}>\underline{k}_{-1}$, most of the molecules are converted to the final state and the concentration of U is very low; thus, the equilibrium between U and N cannot be established. In this case the rate-limiting step is unfolding and the formation of F is determined by first order rate constant, $\underline{k}$:

$$N \xrightarrow{k} F \qquad \text{(SchemeII)}$$

There is another case in which the Lumry–Eyring model can be diminished to two-state model if $\underline{K}=\underline{k}_1/\underline{k}_{-1}<1$ and in addition $\underline{k}_{-1}>\underline{k}$. The amount of U is very low and the rate of formation of F can be determined by an apparent first order rate constant equal to $\underline{K}\underline{k}$. Thus, two-state irreversible model is a limiting case of the Lumry–Eyring model.

Sanchez-Ruiz et al. [19] proposed different methods for estimation of the energy of activation relative for two-state model:

A) The first order rate constant k at given temperature T is:

$$k = vC_p^{ex}/(Q_t - Q) \qquad (1)$$

where v is the scanning rate, C_p^{ex} is the excess heat capacity, Q_t is the enthalpy of denaturation and Q is the heat absorbance up to temperature T.

The rate constant obeys the Arrhenius equation:

$$k = \exp\left[\frac{-E_a}{R}\left(\frac{1}{T^*}-\frac{1}{T}\right)\right] \qquad (2)$$

where $\underline{E}_a$, $\underline{R}$, $\underline{T}$ and $\underline{T}^*$ are activation energy, gas universal constant, absolute temperature and temperature in which $\underline{k}=1\ min^{-1}$, respectively.

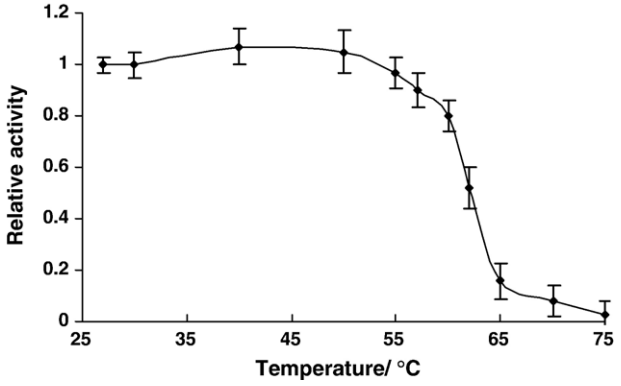

Fig. 1. Relative activity of incubated ELAO in different temperatures for 20 min. The activity was measured at 27 °C.

Taking into consideration these two equations, the following equation is obtained:

$$\frac{1}{T} = \frac{1}{T^*} - \ln[\nu C_p^{ex}/(Q_t - Q)]/(E_a/R) \quad (3)$$

In the plot $1/T$ vs. $\ln[\nu C_p^{ex}/(Q_t - Q)]$ parameters E_a/R and $1/T^*$ can be estimated by the slope and intercept of the plot by $\ln[\nu C_p^{ex}/(Q_t - Q)]$ axis. This method is the most valuable among other methods. If the one step model is valid the $\ln[\nu C_p^{ex}/(Q_t - Q)]$ value is independent of the scanning rate. Therefore points obtained at various scanning rate should be lie on a common line, indeed this plot is one of the criteria suggested by Kurganov for the validity of two-state model [20].

B) The function of enthalpy on temperature has the following form:

$$\ln(\ln[Q/(Q_t - Q)]) = (E_a/R)\left(\frac{1}{T^*} - \frac{1}{T}\right) \quad (4)$$

The ratio E_a/R can be calculated for each scanning rate by the slope of the $\ln(\ln[Q/(Q_t - Q)])$ vs. $1/T$ plot.

Kurganov et al. have obtained the following expression for C_p^{ex} for this model [20]:

$$C_p^{ex} = \frac{1}{\nu}\Delta H \exp\left\{\frac{E_a}{R}\left(\frac{1}{T^*} - \frac{1}{T}\right)\right\} \times \exp\left\{-\frac{1}{\nu}\int_{T_a}^{T} \exp\left[\frac{E_a}{R}\left(\frac{1}{T^*} - \frac{1}{T}\right)\right] dT\right\} \quad (5)$$

The experimental data can be fitted to Eq. (5) to obtain the kinetic parameters. We used the GOSA software for fitting the DSC data for this equation.

2.7. Size-exclusion chromatography

Size exclusion chromatography was performed using a HPLC system (Shimadzu LC-6A) equipped with a shim-pack Diol-300, 7 mm ID × 25 cm, HPLC gel filtration column (Shimadzu Co.). An aliquot of 10 μl of the protein samples (thermal denatured and folded ELAO, 0.2 mg/ml) were injected in to the column mechanically. The column was operated under using flow rate of 0.3 ml/min. The HPLC system set at 278 nm. The elution buffer was 100 mM phosphate buffer, pH 7.0.

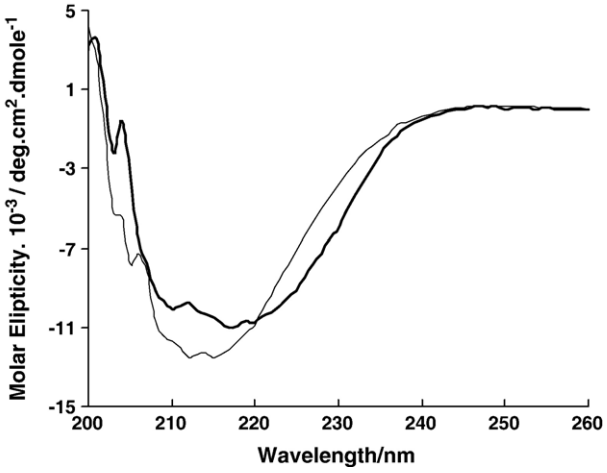

Fig. 2. CD spectra of native (solid line) and thermal denatured (dashed line) ELAO. This experiment was done by 0.25 mg/ml of samples using 0.1 mm cell at 25 °C. The denatured protein was obtained by heating the sample up to 90 °C and then cooling it to room temperature.

3. Results and discussion

Fig. 1 shows the relative activities of ELAO incubated at various temperatures for 20 min and cooled to 27 °C. As can be seen in Fig. 1, ELAO retained its activity up to 55 °C and, above this temperature, lost its activity irreversibly. For further elucidation of irreversible denaturation of ELAO, the CD spectra of native and thermal denatured enzyme were studied at 27 °C. This study was also indicative of irreversibility of denaturation process because the native molar elipticity cannot be regained upon cooling the sample (see Fig. 2). All the mentioned experiments led us to suggest that thermal denaturation of ELAO was an irreversible process and the thermal denatured protein folded back erroneously.

Further experiments with DSC were performed. Fig. 3 shows the DSC profile of ELAO (4 mg/ml) in scanning rate of 1 K/min.

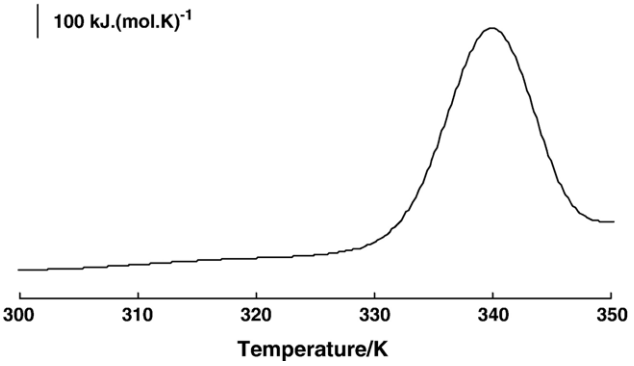

Fig. 3. DSC profile of ELAO (4 mg/ml) in 0.1 M phosphate buffer, pH 7.0, with the scanning rate 1 K/min.

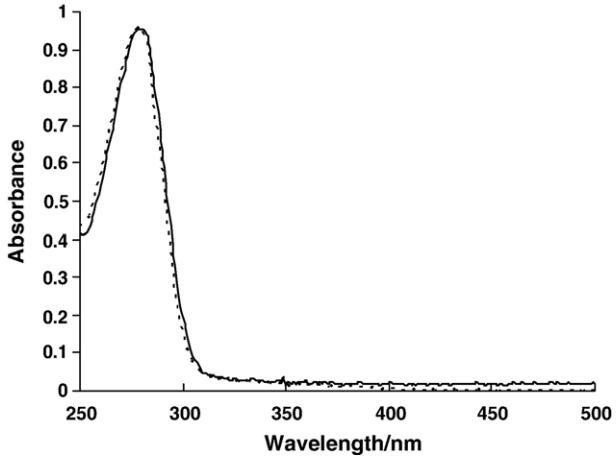

Fig. 4. Changes in absorbance of native (solid line) and thermal denatured (dashed line) ELAO in 0.1 M phosphate buffer, pH 7.0.

When a sample of ELAO was heated at 1–2 °C higher than T_{max} (68 °C) and cooled, the second scanning did not demonstrate a significant thermal effect indicating an irreversible thermal denaturation of ELAO in agreement with the previous results. On the other hand, the absence of any exothermic peak in DSC profile indicated the lack of aggregation in the process. For further confirmation of this suggestion we checked the presence of aggregation by UV/Vis spectroscopy. We heated ELAO sample up to 90 °C and compared its absorbance with native ELAO at 27 °C. As shown in Fig. 4, no significant increase in absorbance in the range 250–500 nm was seen upon thermal denaturation.

Since ELAO is a dimer, one may conclude that thermal denaturation of ELAO can include a step of oligomerization or dissociation to monomers [21]. To elucidate the probability of such effect, we checked the dependence of DSC thermogram on the protein concentration. Our results showed that T_{max} as well as ΔH was not affected by the concentration of the protein in a range

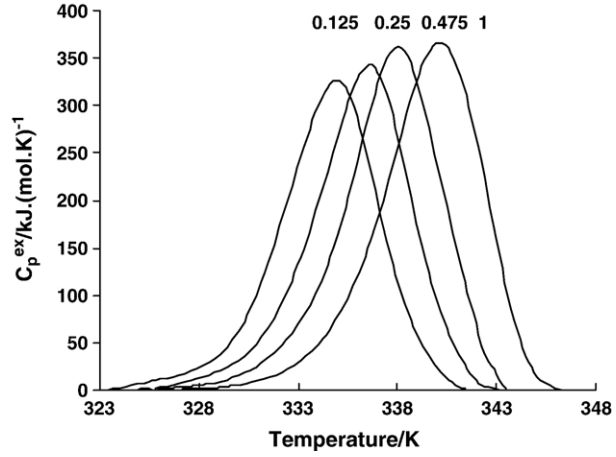

Fig. 5. Temperature dependence of excess heat capacity of ELAO in 0.1 M phosphate buffer, pH 7.0, at various scanning rates as indicated. In all scanning rates the protein concentrations were 1 mg/ml.

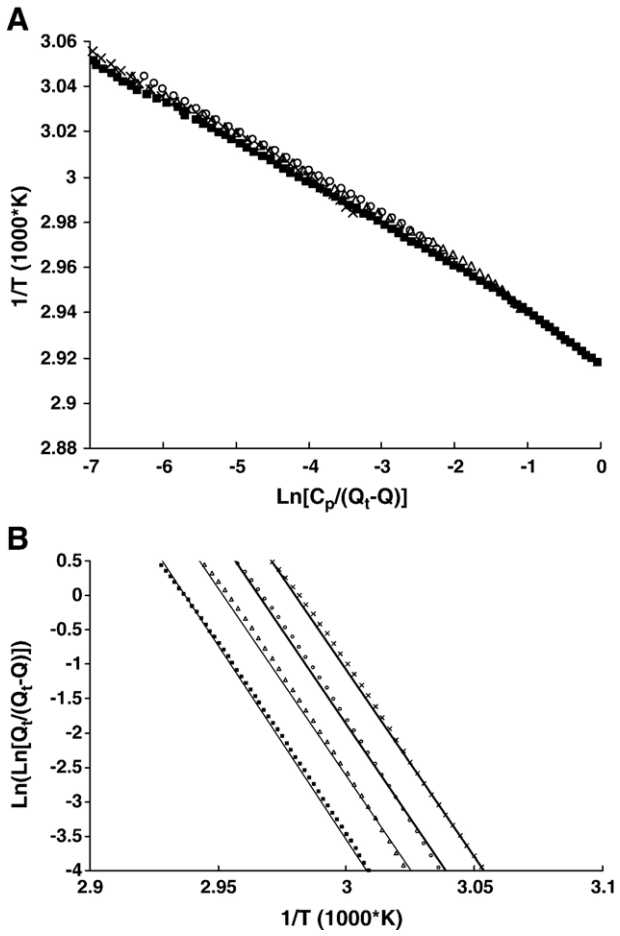

Fig. 6. Graphical methods of analysis of the DSC profiles. (A) Dependence of $1/T$ on $\ln[vC^{ex}_p/(Q_t - Q)]$ for ELAO based on Eq. (3). The linearity and overlapping of this plot at various scanning rates verifies the validity of the two-state model for this enzyme. (B) Plot of heat evolved according to Eq. (4) at various scanning rates. ■, Δ, ○, × stand for 1, 0.475, 0.25, and 0.125 K/min scanning rate, respectively.

of 0.5–4.0 mg/ml. It was significant that oligomerization did not contribute in thermal denaturation of ELAO. Performed DSC experiments at varied scanning rates (Fig. 5) showed that the T_{max} value was affected by heating rates and, as the heating rate increased, T_{max} shifted towards higher temperatures showing that ELAO denaturation was kinetically controlled. Independence of the thermodynamic parameters of the protein concentration and lack of aggregation allowed us to suggest that thermal denaturation of ELAO may obey the two-state model. Although there are some proteins which is aggregated during thermal denaturation and still two-state model is validate for their behavior [22]. The validity of this model was then verified by plots of ln $(vC^{ex}_p/(Q_t - Q))$ vs. $1/T$ at different scanning rates (Fig. 6A). The

Table 1
Calculated values based on Eqs. (3) and (4)

Equation used	E_a, kJ/mol	SD	T^*, Ks	SD
Eq. (3)	454	8	341.8	0.4
Eq. (4)	454	2		

Slopes and intercept are obtained from trend lines of curves in Fig. 4.
* SD stands for standard deviation.

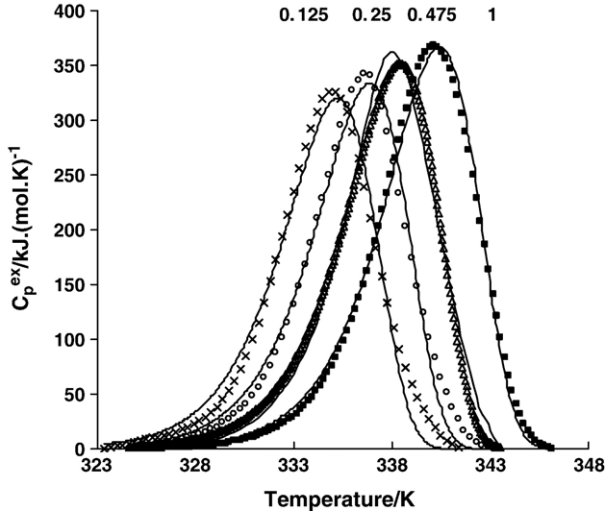

Fig. 7. DSC profiles of ELAO (2 mg/ml) in 0.1 M phosphate buffer, pH 7.0, at various scanning rates. The continuous lines show the fitted curves using GOSA software. ■, Δ, ○, × stand for 1, 0.475, 0.25, and 0.125 K/min scanning rate, respectively.

overlap of curves and their linearity showed that the two-state model can explain thermal denaturation of ELAO [20]. We used the graphical methods (see Material and methods) to calculate parameters E_a and $\underline{T}$*. Fig. 6A and B show the profiles based on Eqs. (3) and (4), and the values parameters calculated according to these methods are given in Table 1.

We also used GOSA software to fitting Eq. (5) to the DSC experimental data (see Fig. 7). The results of this fitting, presented in Table 2, demonstrate agreement between obtained parameters from fitting and graphical methods. The differences can be explained by the fact that, when applying Eqs. (3) and (4), we used the experimental points in range of the $\frac{Q}{Q_t}$ values from 5 to 95% because of large distortions on the initial and final parts of the typical DSC curves, which could result in a systematic error in estimation of parameters [23], while in fitting Eq. (5) to the experimental data we used all range of the $\frac{Q}{Q_t}$ values. The calculated experimental total enthalpy of the unfolding process displayed an average value being 2126± 136 kJ/mol or 15.2± 1.0 J/g. This value of specific enthalpy was located between enthalpy expected by Lyubarev and Kurganov [23]. According to their opinion, most of proteins that undergoing thermal denaturation by the one-step model, can be divided into two groups:

A) Proteins which denaturate at 40–60 °C with specific enthalpy in range of 12–15 J/g.
B) Proteins which denaturate at 60–80 °C with specific enthalpy in range of 18–23 J/g.

Based on the Poltorak method [24,25], the following model may be proposed for thermal denaturation of ELAO:

$$E_2 \underset{k_{-1}}{\overset{k_1}{\rightleftharpoons}} 2E \overset{k_{den}}{\rightarrow} 2E_{den} \qquad \text{(SchemeIII)}$$

where k_1, k_{-1}, and k_{den} are the rate constants for the forward and backward stages of dissociation and the stage of denaturation, respectively. E_1, E_2, and E_{den} represent the monomeric, dimeric, and denatured forms of the enzyme. If denaturation is rapid in comparison with dissociation of dimer and association of monomer ($k_{den} > k_1$ and $k_{den} > k_{-1}$), the kinetics of denaturation of dimeric protein can be described by the two-state model [22] as follows:

$$E_2 \overset{k}{\rightarrow} 2E_{den} \qquad \text{(SchemeIV)}$$

For further discrimination in models we made HPLC experiments to show the dimeric state of the denatured protein. HPLC experiments showed that the retention time for denatured ELAO (22.7 min) was less than that for the folded state (23.9 min), indicative of a dimeric state of the denatured protein while it became somehow more expanded during denaturation. So we proposed for ELAO denaturation the two-state irreversible model:

$$E_2 \overset{k}{\rightarrow} E_{2,den} \qquad \text{(SchemeV)}$$

How can we explain these discrepancies? The answer is that the Poltorak method is fundamentally based on assumption that in some oligomeric enzymes only the dimeric form is active and their monomeric components are inactive. It may arise from the contribution of inter-protein contacts in forming the active site [24,25]. Now we assume that there are other more stable inter-protein contacts not contributing in forming the active site. Thus, thermal denaturation can disrupt the active site by breaking those contacts which are important for activity but other interface contacts are still intact. In order to explain these experimental data and to confirm the contact which does not contribute in conformational lock structure in ELAO, we used the X-ray crystallography structure of PSAO [26] as a model because nucleotide sequence alignment of ELAO vs. PSAO showed about 90% sequence identities and 93% homology [25]. PSAO has two structurally identical subunits, each is composed of three domains called D2, D3 and D4 [27]. If PSAO is shaped like a mushroom, the major part of molecule forms the cap of mushroom and a short stalk is made by the C-terminal of subunits. A cysteinyl residue, Cys647, is located two residues before the C-terminal in the stalk. Titration of substrate-reduced

Table 2
Values of parameters obtained from fitting based on Eq. (5) to the experimental data using GOSA software

Scan rate, K/min	0.125			0.25			0.475			1		
Parameter	$\underline{T}$*, K	$\underline{E}_a$, kJ/mol	$\Delta\underline{H}$, kJ/mol	$\underline{T}$*, K	$\underline{E}_a$, kJ/mol	$\Delta\underline{H}$, kJ/mol	$\underline{T}$*, K	$\underline{E}_a$, kJ/mol	$\Delta\underline{H}$, kJ/mol	$\underline{T}$*, K	$\underline{E}_a$, kJ/mol	$\Delta\underline{H}$, kJ/mol
Value	342.1	403	1981	342.1	407	2057	342.00	411	2181	342.45	408	2318
SD[a]	0.15	7	27	0.1	6	25	0.08	6	26	0.03	3	13

[a] SD stands for standard deviation.

PSAO and ELAO with a variety of reagents have so far failed to provide evidence for free cysteine [26,27]. Alignment of the C-terminal shows that VACPGCSN sequence is similar in ELAO and PSAO. The lack of detectable free cysteines in PSAO and ELAO can be rationalized by the formation of inter-subunit disulfide bond. The evidence for disorder at the three C-terminal residues in PSAO is inconsistence with the presence of such a bond in the PSAO structure but the cysteines of the two subunits could be brought within S–S bonding distance if the configuration at the proline residue is changed from *trans* to *cis*. The possibility that it may occur, particularly following partial unfolding, has not been eliminated [26]. So this probable formed S–S bond can link two unfolded monomer as a hinge and conserves unfolded state of ELAO in dimeric form.

4. Conclusion

Activity measurement as well as CD spectropolarometry show that thermal denaturation of ELAO is an irreversible process. DSC studies are also consistent with these results. Absence of aggregation and checking of the validity of the two-state model by $\ln[\nu C_p^{ex}/(Q_t - Q)]$ vs. $1/T$ plots at various scanning rates enable us to conclude that the two-state model satisfy thermal denaturation of ELAO. Based on this model we estimate the activation energy, parameter T^* (the absolute temperature at which the rate constant of denaturation is equal to 1 min^{-1}), and total enthalpy of ELAO denaturation. HPLC experiments show that thermal denatured ELAO conserves its dimeric state. Finally crystallographic data and experiments on sulfhydryl detection show the possibility of inter-subunit S–S bond formation at C-terminal position which may link two denatured monomer. The following model for thermal denaturation of ELAO is, therefore, proposed:

$$N_2 \xrightarrow{k} D_2$$

where N_2 and D_2 are the native and denatured dimer, respectively.

Acknowledgements

Financial support provided from the Research Council of the University of Tehran and Iran National Science Foundation (INSF) are gratefully appreciated. This study was also partly supported by 60% funds from Cagliari University, Italy.

References

[1] N.K. Williams, J.P. Klinman, Whence topa? Models for biogenesis of topa quinone in copper amine oxidase, J. Mol. Catal., B Enzym. 8 (2000) 95–101.
[2] F. Boosman, J. van Dijk, U.M. Bhaggoe, A.M. Bouhuzien, A.H. van den Meiracker, Variation in semicarbazide-sensitive amine oxidase activity in plasma and tissues of mammals, Comp. Biochem. Physiol., C-Toxicol. Pharmacol. 126 (2000) 69–78.
[3] P. Yu, D.M. Zuo, Oxidative deamination of methylamine by semicarbazide-sensitive amine oxidase leads to cytotoxic damage in endothelial cells, Diabebetes 42 (1993) 594–603.
[4] F. Boomsman, P.J. de Kam, G. Tjeerdsma, A.H. van den Meiracker, D.J. van Veldhuisen, Plasma semicarbazide-sensitive amine oxidase (SSAO) is an independent prognostic marker for mortality in chronic heart failure, Eur. Heart J. 21 (2000) 1859–1863.
[5] R. Lewinsohn, Mammalian monoamine oxidizing enzymes with special reference to benzylaminase in human tissue, Braz. J. Biol. Res. 17 (1984) 223–256.
[6] T.A. Smith, The di and poliamine oxidases of higher plants, Biochem. Soc. Trans. 13 (1985) 319–322.
[7] H.E. Flores, P. Filner, Putrescine catabolism in plant cells: γ-amino butyraldehyde dehydrogenase activity in mono and dicotyledonous species, Plant Physiol. 75 (1984) 670.
[8] A.R. Cona, R. Angelini, R. Federico, A preliminary study of hormonal regulation of diamine oxidase activity in lentil seedlings, Ann. Bot. 46 (1987) 135–141.
[9] P. Joseph, S.K. Srivastava, Photoregulation of diamine oxidases from pea seedling, J. Plant Physiol. 146 (1995) 108–114.
[10] M. Maccarrone, A. Rossi, L. Avigliano, A. Finazzi Agrò, Activity and expression of diamine oxidase in lentil seedlings under different growth condition, Plant Sci. 79 (1991) 51–55.
[11] S. Das, A. Bose, B. Ghosh, Effects of salt stress on polyamine metabolism in *Brassica campestris*, Phytochemistry 39 (1995) 283–285.
[12] M. Scalet, R. Federico, R. Angelini, Time courses of diamine oxidase and peroxidase activities and polyamine changes after mechanical injury of chick-pea seedlings, J. Plant Physiol. 137 (1991) 571–575.
[13] G. Rea, O. Metoui, A. Infantino, R. Federico, R. Angelini, Copper amine oxidase expression in defense responses to wounding and *Ascochyta rabiei* invasion, Plant Physiol. 128 (2002) 865–875.
[14] S.Z. Moosavi-Nejad, M. Rezaei-Tavirani, A. Padiglia, G. Floris, A.A. Moosavi-Movahedi, Amine oxidase from lentil seedlings: energetic domains and effect of temperature on activity, J. Protein Chem. 20 (2001) 405–411.
[15] A. Giartosio, E. Agostinelli, B. Mondovì, Domains in bovine serum amine oxidase, Biochem. Biophys. Res. Commun. 154 (1988) 66–72.
[16] E. Agostinelli, L. Morpurgo, C. Wang, A. Giartosio, B. Mondovi, Properties of cobalt-substituted bovine serum amine oxidase, Eur. J. Biochem. 222 (1994) 727–732.
[17] A. Padiglia, R. Medda, A. Lorrai, B. Murgia, J.Z. Pedersen, A. Finazzi Agrò, G. Floris, Characterization of *Euphorbia characias* latex amine oxidase, Plant Physiol. 117 (1998) 1363–1371.
[18] A. Rinaldi, G. Floris, A. Finazzi Agrò, Purification and properties of diamine oxidase from *Euphorbia* latex, Eur. J. Biochem. 127 (1982) 417–422.
[19] J.M. Sanchez-Ruiz, J.L. Lopez-Lacomba, M. Cortijo, P.L. Mateo, Differential scanning calorimetry of the irreversible thermal denaturation of thermolysin, Biochemistry 27 (1988) 1648–1652.
[20] B.I. Kurganov, A.E. Lyubarev, J.M. Sanchez-Ruiz, V.L. Shnyrov, Analysis of differential scanning calorimetry data for proteins. Criteria of validity of one-step mechanism of irreversible protein denaturation, Biophys. Chemist. 69 (1997) 125–135.
[21] K. Takahashi, J.M. Sturtevant, Thermal denaturation of Streptomyces subtilisin inhibitor, subtilisin BPN′, and the inhibitor–subtilisin complex, Biochemistry 20 (1981) 6185–6190.
[22] A.E. Lyubarev, B.I. Kurganov, V.N. Orlov, H.M. Zhou, Two-state irreversible thermal denaturation of muscle creatine kinase, Biophys. Chemist. 79 (1999) 199–204.
[23] A.E. Lyubarev, B.I. Kurganov, Study of irreversible thermal denaturation of proteins by differential scanning calorimetry, Recent Res. Dev. Biophys. Chem. 2 (2001) 141–165.
[24] O.M. Poltorak, E.S. Chukhray, I.Y. Torshin, Dissociative thermal inactivation, stability, and activity of oligomeric enzymes, Biochemistry (Moscow) 63 (1998) 303–311.
[25] M. Amani, A.A. Moosavi-Movahedi, G. Floris, S. Longu, A. Mura, S.Z. Moosavi-Nejad, A.A. Saboury, F. Ahmad, Comparative study of the conformational lock, dissociative thermal inactivation and stability of *Euphorbia* latex and lentil seedling amine oxidases, Protein J. 24 (2005) 183–191.
[26] V. Kumar, D.M. Dooley, H.C. Freeman, J.M. Guss, I. Harvey, M.A. McGuirl, M.C.J. Wilce, V.M. Zubak, Crystal structure of a eukaryotic (pea seedling) copper-containing amine oxidase at 2.2 A resolution, Structure 4 (1996) 943–955.
[27] G. Floris, A. Giartosio, A. Rinaldi, Essential sulfhydryl groups in diamine oxidase from *Euphorbia characias* latex, Arch. Biochem. Biophys. 220 (1983) 623–627.